Title: Testing Gravity Using Type Ia Supernovae Discovered by Next-Generation Wide-Field Imaging Surveys

Thematic Science Area: Cosmology and Fundamental Physics

Authors: and a list of authors

Lead Author Contact Information: Alex Kim; Physics Division, Lawrence Berkeley National Laboratory, 1 Cyclotron Road, Berkeley, CA, 94720; 1-510-486-4621; agkim@lbl.gov

Draft version January 28, 2019
Typeset using LaTeX default style in AASTeX62

Testing Gravity Using Type Ia Supernovae Discovered by Next Generation Wide Field Imaging Surveys

A. G. Kim,[1] G. Aldering,[1] P. Antilogus,[2] S. BenZvi,[3] H. Courtois,[4] T. Davis,[5] S. Gontcho A Gontcho,[3] R. Graziani,[6] C. Harper,[1] C. Howlett,[7] D. Huterer,[8] C. Ju,[1] P.-F. Leget,[2] E. V. Linder,[1] P. McDonald,[1] J. Nordin,[9] S. Perlmutter,[1,10] N. Regnault,[2] M. Rigault,[4] A. Složar,[11] and others

[1] *Physics Division, Lawrence Berkeley National Laboratory, 1 Cyclotron Road, Berkeley, CA, 94720*
[2] *Laboratoire de Physique Nucléaire et de Hautes Energies, Sorbonne Université, CNRS-IN2P3, 4 Place Jussieu, 75005 Paris, France*
[3] *Department of Physics and Astronomy, University of Rochester, Rochester, NY 14627, USA*
[4] *Université de Lyon, F-69622, Lyon, France; Université de Lyon 1, Villeurbanne; CNRS/IN2P3, Institut de Physique Nuclaire de Lyon, France*
[5] *School of Mathematics and Physics, University of Queensland, Brisbane, QLD 4072, Australia*
[6] *Université Clermont Auvergne, CNRS/IN2P3, Laboratoire de Physique de Clermont, F-63000 Clermont-Ferrand, France*
[7] *International Centre for Radio Astronomy Research, The University of Western Australia, Crawley, WA 6009, Australia*
[8] *Department of Physics, University of Michigan, 450 Church Street, Ann Arbor, MI 48109, USA*
[9] *Institut fur Physik, Humboldt-Universitat zu Berlin, Newtonstr. 15, 12489 Berlin, Germany*
[10] *Department of Physics, University of California Berkeley, 366 LeConte Hall MC 7300, Berkeley, CA, 94720-7300*
[11] *Brookhaven National Laboratory, Physics Department, Upton, NY 11973, USA*

ABSTRACT

In the upcoming decade cadenced wide-field imaging surveys will increase the number of identified $z < 0.3$ Type Ia supernovae (SNe Ia) from the hundreds to the hundreds of thousands. The increase in the number density and solid-angle coverage of SNe Ia, in parallel with improvements in the standardization of their absolute magnitudes, now make them competitive probes of the growth of structure and hence of gravity. The peculiar velocity power spectrum is sensitive to γ, which captures the effect of gravity on the linear growth of structure through the relation $f = \Omega_M^\gamma$. In the next decade the peculiar velocities of SNe Ia in the local $z < 0.3$ Universe will provide a measure of γ with as low as 0.01 precision that can definitively distinguish between General Relativity and leading models of alternative gravity.

1. INTRODUCTION

In the late 1990's, Type Ia supernovae (SNe Ia) were used as distance probes to measure the homogeneous expansion history of the Universe. The remarkable discovery that the expansion is accelerating has called into question our basic understanding of the gravitational forces within the Universe. Either it is dominated by a "dark energy" that is gravitationally repulsive, or General Relativity is inadequate and needs to be replaced by a modified theory of gravity. It is only appropriate that in the upcoming decade, with their sheer numbers, solid-angle coverage, and improved distance precisions, SNe Ia will provide measurements of the *inhomogeneous* motions of structures in the Universe that will provide an unmatched test of whether dark energy or modified gravity is responsible for the accelerating expansion of the Universe.

In the next decade, SNe Ia will be used as peculiar-velocity probes to measure the influence of gravity on structure formation within the Universe. The peculiar velocity power spectrum is sensitive to the growth of structure as $P_{vv} \propto (fD)^2$, where D is the linear growth factor and $f \equiv \frac{d\ln D}{d\ln a}$ is the linear growth rate (Hui & Greene 2006; Davis et al. 2011).[1] The ΛCDM prediction for the $z = 0$ peculiar velocity power spectrum is shown in Figure 1. The growth of structure depends on gravity, indeed Linder & Cahn (2007) find that General Relativity, $f(R)$, and DGP gravities follow the relation $f \approx \Omega_M^\gamma$ with $\gamma = 0.55, 0.42, 0.68$ respectively. Adopting this parameterization to model gravity, peculiar velocity surveys are sensitive to $fD = \Omega_M^\gamma \exp\left(\int_a^1 \Omega_M^\gamma d\ln a\right)$, whose prediction for ΛCDM is plotted in Figure 2 of Linder (2013).[2]

[1] To be precise, the peculiar velocity power spectrum also depends on the Hubble parameter as $P_{vv} \propto (HfD)^2$. A supernova survey measures luminosity distance fluctuations $\delta_{d_L} = (d_L - \bar{d}_L(z))/\bar{d}_L(z)$, where d_L is the observed distance and $\bar{d}_L(z)$ is the expected distance at the observed redshift z. To first order in peculiar velocity along the line of sight v, $\delta_{d_L} = v\left(1 - \frac{1}{H\bar{d}_L(z)}\right) \approx -\frac{v}{H\bar{d}_L(z)}$ at low redshift. The H-dependences of P_{vv} and the conversion from distances to velocities cancel, making peculiar velocity surveys sensitive to $(fD)^2$.

[2] The parameter σ_8, the standard deviation of overdensities in $8h^{-1}$Mpc spheres, is commonly used in place of D to normalize the overall amplitude of overdensities, so the standard parameterization used by the community is $f\sigma_8$.

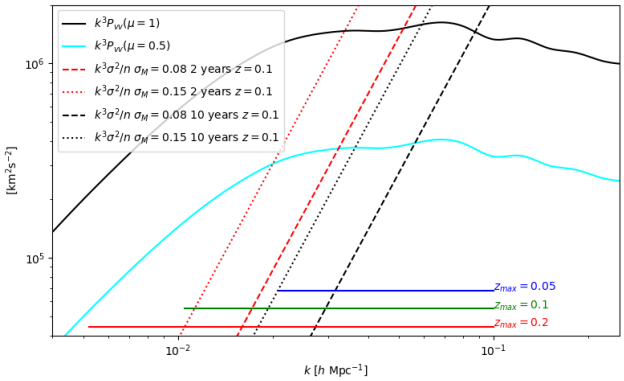

Figure 1. Volume-weighted peculiar velocity power spectrum $k^3P_{vv}(z=0)$ for $\mu=1, 0.5$ (solid black, cyan) as predicted for General Relativity in the linear regime. Overplotted are volume-weighted peculiar velocity shot-noise $k^3\sigma^2/n$ at $z=0.1$ expected from 2- and 10-year (red, black) supernova densities, 0.08 and 0.15 mag (dashed, dotted) intrinsic magnitude dispersions. The bottom solid horizontal lines show the approximate range of k expected to be used in surveys with corresponding redshift depths z_{max}.

Peculiar velocity surveys have already been used to measure fD, though not to a level where gravity models can be precisely distinguished. Adams & Blake (2017) use 6dFGS peculiar velocities using the Fundamental Plane method to get a 15% uncertainty in fD at $z\approx 0$ using combined density and velocity information. The upcoming TAIPAN survey will obtain Fundamental Plane galaxies with densities of $n_g\sim 10^{-3}h^3\,\mathrm{Mpc}^{-3}$, and the WALLABY+WNSHS surveys will obtain Tully-Fisher galaxies at densities $n_g\sim 2\times10^{-2}-10^{-4}h^3\,\mathrm{Mpc}^{-3}$ from $z=0-0.1$ covering 75% of the sky. These surveys combined are projected to have 3% fD uncertainties (Howlett et al. 2017b). (For reference, DESI projects 10% precision of fD at $z\approx 0.3$ using Redshift Space Distortions (RSD) alone.) Existing SN Ia samples have been used to test and ultimately find spatial correlations in peculiar velocities that may be attributed to the growth of structure (Gordon et al. 2007; Abate & Lahav 2008; Johnson et al. 2014; Huterer et al. 2015, 2017).

Two advances in the upcoming decade will make SN Ia peculiar velocities more powerful. First, the precision of SN Ia distances can be improved. The commonly-used empirical 2-parameter SED model yields $\sigma_M\gtrsim 0.12$ mag absolute magnitude dispersion. However, SNe transmit more information than just the light-curve shape and single color used in current SN models. Recent studies indicate that with the right data, SN absolute magnitudes can be calibrated to $\sigma_M\lesssim 0.08$ mag (see e.g. Barone-Nugent et al. 2012; Fakhouri et al. 2015). Though not yet established, it is anticipated that such a reduction in intrinsic dispersion comes with a reduction in the magnitude bias correlated with host-galaxy properties that is observed using current calibrations. One such SN is worth $\gtrsim 25$ galaxies with 0.4 mag absolute magnitude uncertainty. Secondly, in the upcoming decade cadenced wide-field imaging surveys such as ZTF and LSST will increase the number of identified $z<0.3$ Type Ia supernovae (SNe Ia) from the hundreds to the hundreds of thousands; over the course of 10-years, LSST will find $\sim 150,000$ $z<0.2$, $\sim 520,000$ $z<0.3$ SNe Ia for which good light curves can be measured, corresponding to a number density of $n\sim 5\times10^{-4}h^3\,\mathrm{Mpc}^{-3}$. This sample has comparable number density and more galaxies at deeper redshifts than projected by WALLABY and TAIPAN.

Given these two advances, supernovae discovered by wide-field searches in the next decade will measure the growth of structure. For example, over the course of a decade an LSST SN survey can produce find 4–14% uncertainties in fD in 0.05 redshift bins from $z=0$ to 0.3, cumulatively giving 2.2% uncertainty on fD within this interval , where at $0<z<0.2$ most of the probative power comes from peculiar velocities and at higher redshifts from *RSD* (Howlett et al. 2017a).

2. TESTING GRAVITY WITH PECULIAR VELOCITY SURVEYS

While the growth rate fD can be used to test several aspects of physics beyond the standard cosmological model (e.g. dark matter clustering, dark energy evolution), our scientific interest here is in probing gravity so we here focus on γ. To illustrate the distinction, $\frac{d(\ln fD)}{d\gamma}=\ln\Omega_M+\int\Omega_M^\gamma\ln\Omega_M\,d\ln a\approx -1.68,-0.75,-0.37$ at $z=0,0.5,1.0$ respectively in ΛCDM; two surveys with the same fractional precision in fD will have different precision in γ, with the one at lower redshift providing the tighter constraint. We project uncertainties in γ, σ_γ for a suite of idealized surveys using

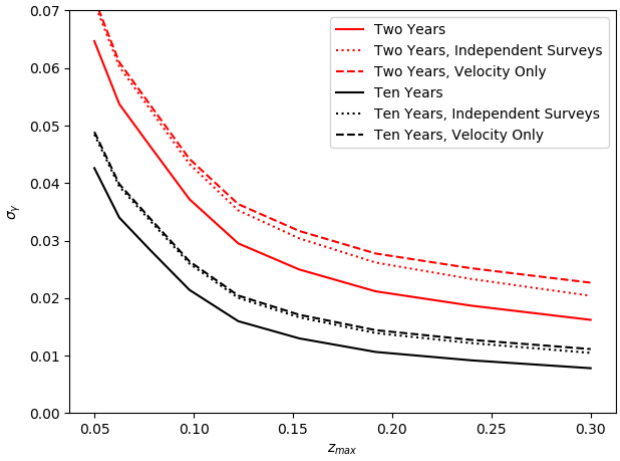

Figure 2. The projected uncertainty in γ, σ_γ, achieved by two- (red) and ten-year (black) surveys of varying depth z_{max}. For each survey uncertainties are based on three types of analyses, one that only uses peculiar velocities (dashed), one that uses both RSD and peculiar velocities independently (dotted), and one that uses both RSD, peculiar velocities, and their cross-correlation (solid).

a Fisher matrix analysis similar to that of Howlett et al. (2017a,b). The Fisher information matrix is

$$F_{ij} = \frac{\Omega}{8\pi^2} \int_0^{r_{max}} \int_{k_{min}}^{k_{max}} \int_{-1}^{1} r^2 k^2 \mathrm{Tr}\left[C^{-1} \frac{\partial C}{\partial \lambda_i} C^{-1} \frac{\partial C}{\partial \lambda_j} \right] d\mu\, dk\, dr \tag{1}$$

where

$$C(k,\mu) = \begin{bmatrix} P_{\delta\delta}(k,\mu) + \frac{1}{n} & P_{v\delta}(k,\mu) \\ P_{v\delta}(k,\mu) & P_{vv}(k,\mu) + \frac{\sigma^2}{n} \end{bmatrix} \tag{2}$$

and the two parameters considered are $\lambda \in \{\gamma, bD\}$. The parameter dependence enters through $(fD)(\gamma)$ in the relations $P_{vv} \propto (fD\mu)^2$, the SN Ia host-galaxy overdensity power spectrum $P_{\delta\delta} \propto (bD + fD\mu^2)^2$, and the galaxy-velocity cross-correlation $P_{vg} \propto (bD + fD\mu^2) fD$, where b is the galaxy bias and μ is the cosine of the angle between the k-mode and the line of sight. While the bD term does contain information on γ, its constraining power is not used here. The uncertainty in γ is $\sigma_\gamma = \sqrt{(F^{-1})_{\gamma\gamma}}$. Non-GR models may also predict a change in the scale-dependence of the growth or non-constant γ, such observations provide additional leverage in probing gravity but are not considered.

The uncertainty σ_γ of a survey depends on its solid angle Ω, depth $r_{max} = \chi(z_{max})$, duration t through $n = \epsilon\phi t$ where ϕ is the observer-frame SN Ia rate and ϵ is the sample-selection efficiency, and the intrinsic SN Ia magnitude dispersion through $\sigma \approx (\frac{5}{\ln 10}\frac{1+z}{z})^{-1}\sigma_M$. An analysis in which the RSD and velocity surveys are treated independently sets the off-diagonal elements of C to zero.

We consider peculiar velocity surveys for a range of redshift depths z_{max} for survey durations of $t = 2$ and 10 years. The other survey parameters $\Omega = 3\pi$, $\epsilon = 0.65$, $\sigma_M = 0.08$ mag are fixed. The k-limits are taken to be $k_{min} = \pi/r_{max}$ and $k_{max} = 0.1\ h\,\mathrm{Mpc}^{-1}$. The sample-selection efficiency ϵ is redshift-independent, i.e. the native redshift distribution is not sculpted. The input bias of SN Ia host galaxies is set as $b = 1.2$.

All the surveys considered provide meaningful tests of gravity. The projected uncertainty in γ achieved by the suite of surveys are shown in Figure 2. The primary analysis of interest uses overdensities (RSD), peculiar velocities, and their cross-correlations. The short and shallow, 2-year, $z_{max} = 0.1$ survey has $\sigma_\gamma \sim 0.038$, which can distinguish between General Relativity, $f(R)$, and DGP gravities at the $> 3\sigma$ level. The 10-year survey performance asymptotes at $z_{max} \sim 0.2$ at a precision of $\sigma_\gamma \sim 0.01$. Figure 2 also shows uncertainties based on two other analyses, one that only uses peculiar velocities, and one that uses both RSD and peculiar velocities independently. Peculiar velocities alone can account for much of the probative power of the surveys. RSD alone do not provide significant constraints. However, considering RSD and velocity cross-correlations decreases σ_γ by $\sim 20\%$. The implication is that there are important k-modes that are sample variance limited either in overdensity and/or peculiar velocity who benefit from the sample-noise suppression engendered by cross-correlations.

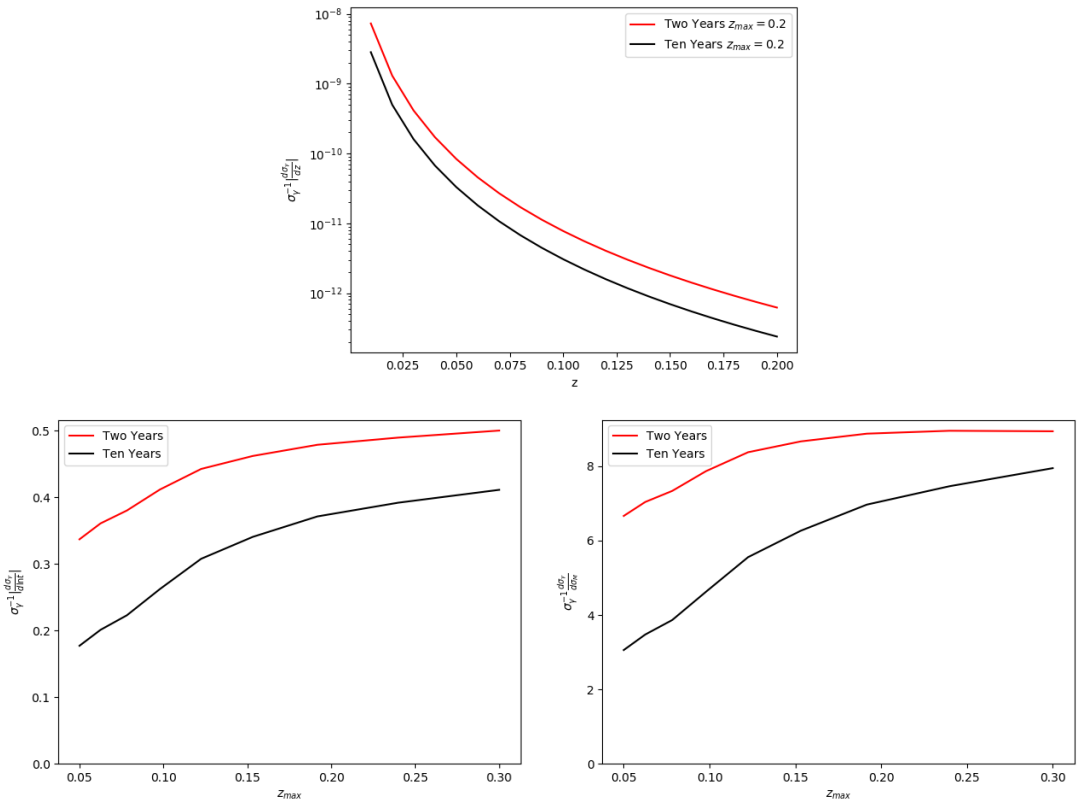

Figure 3. Top: $|\partial\sigma_\gamma/\partial z|$ after two and ten years for a survy with limiting depth $z_{max} = 0.2$. Bottom Left: $\sigma_\gamma^{-1}|\partial\sigma_\gamma/\partial \ln t|$; Bottom Right: $\sigma_\gamma^{-1}\partial\sigma_\gamma/\partial\sigma_M$ each as a function of z_{max} for two- and ten-year surveys.

Survey performance is examined in more detail by considering how σ_γ (using RSD, peculiar velocities, and their cross-correlations) changes with respect to the survey parameters Ω, z_{max}, t, and σ_M, and also with respect to differential redshift bins within a given survey. Though not directly a survey parameter, we also examine changes with respect to k_{max}.

Solid Angle Ω: The Fisher Matrix F is proportional to the survey solid angle Ω so $\sigma_\gamma \propto \Omega^{-1/2}$.

Differential Redshift Bin z: Certain redshifts constrain γ more strongly than others. If at a given moment of a survey we had a set of SNe Ia from which to choose, it turns out the one with the lowest redshift would be preferred. This is demonstrated to be the case at the end of both 2- and 10-year surveys with $z_{max} = 0.2$. The top panel of Figure 3 shows $|\partial\sigma_\gamma/\partial z|$, which for both surveys monotonically decreases from $z = 0.01$ out to $z = 0.2$. If we had to sculpt the distribution (say due to limited follow-up resources), the preference would be to cut out the highest redshift bins resulting in a decreased z_{max}. The optimal redshift distribution is thus the unsculpted SN-discovery distribution truncated by z_{max}.

Redshift Depth z_{max}: Increasing the survey redshift depth increases the γ precision. The differential improvement in σ_γ plateaus at $z_{max} \sim 0.2$ as seen in Figure 2.

Survey duration t; Intrinsic Magnitude Dispersion σ_M: Increasing the survey duration increases the number density of discovered supernovae. The increased survey duration improves the precision in γ as shot-noise is relevant for all the surveys considered. The surveys with the highest fractional benefit are those that are more susceptible to shot noise: those that monitor higher redshifts that have higher velocity dispersion, and shorter surveys due to their lower number densities. These trends are shown in the bottom-left panel of Figure 3, which plots $\sigma_\gamma^{-1}|\partial\sigma_\gamma/\partial \ln t|$ as a function of z_{max} for two- and ten-year surveys. Like survey duration, intrinsic magnitude dispersion is related to survey performance through the shot noise and thus has a similar relationship with σ_γ. This is evident in the plot of $\sigma_\gamma^{-1}\partial\sigma_\gamma/\partial\sigma_M$ shown in the bottom-right panel of Figure 3.

Minimum length scale, maximum wavenumber k_{max}: There is a minimum length scale at which density and velocity distributions are reliably predicted from theory. Changes in this scale engender fractional changes in the γ precision as $\sigma_\gamma^{-1}\partial\sigma_\gamma/\partial k_{max} = 0.0050$ at $k_{max} = 0.1h\,\mathrm{Mpc}^{-1}$, which is survey-independent.

From the above calculations, we find empirically that shot noise is important but that sample variance is non-negligible toward the end of longer surveys or when the intrinsic magnitude dispersion is small. Fine tuning survey design is aided by understanding when surveys become sample variance limited. After a few years the RSD measurement is sample variance limited, the rest-frame volumetric SN Ia rate is $\phi = 7.84 \times 10^{-5} h^3\,\mathrm{Mpc}^{-3}\,\mathrm{yr}^{-1}$. For peculiar velocities, the contributions of P_{vv} and σ^2/n at $z = 0.1$ for $\sigma_M = 0.08, 0.15$ mag with number densities from 2- and 10-year surveys can be compared using Figure 1. For these survey scenarios, sample variance and shot-noise equality occurs at a k within the range that carries the most signal; both sample variance and shot-noise limited modes contribute to the constraints. If k_{max} were to decrease moderately some of the surveys could become sample variance limited, whereas increases in k_{max} introduce additional shot-limited modes.

3. COMPONENTS AND CONSIDERATIONS OF A PECULIAR VELOCITY SURVEY

In the above we have established how survey performance depends on the parameters Ω, z_{max}, t, and σ_M. We now touch on how survey elements affect Ω, z_{max}, and σ_M.

- Spectroscopic transient classification: SNe Ia are defined based on spectroscopic features, through the absence of Hydrogen and the presence of the 6150 Å Silicon P-Cygni feature. Maintaining a low sample intrinsic magnitude dispersion σ_M relies on a the survey having spectroscopic classification to provide a pure sample (e.g. SNIFS, SED Machine; the low surface density of active low-z transients makes MOS superfluous). Photometric classification is an alternative survey choice, and the amount of sample dispersion that can be achieved photometrically is an active subject of research. Photometric classification benefits from having spectroscopic redshifts.

- Spectroscopic redshifts: Peculiar velocities are extracted directly from redshift measurements. Redshift uncertainties of $> 0.5\%$ contribute significantly to the error budget. We thus conclude that there is the need for spectroscopic $R > 200$ host-galaxy redshifts. These redshifts could come as a natural byproduct of the spectroscopic transient classification if the spectrograph has sufficient resolution. Alternatively, moderate-resolution (bright-)galaxy redshift surveys (e.g. DESI, 4MOST) can provide multiplexed observations of a significant fraction of nearby SN hosts before discovery or after transient light has faded away.

- Rolling imaging surveys: SNe Ia must be discovered and their distances determined. Wide-field cadenced imaging surveys (e.g. ZTF, LSST) can deliver both, though there is a question as to distances will be derived solely from the light curves they generate. For example, LSST is expected to discover all $z < 0.3$ SNe Ia before maximum light in its active Wide Fast Deep (WFD) survey area. The nominal cadence produces sparse per-band light curves with limited ability to constrain distances. The observing strategy of the imaging survey thus has a trade between the solid angle (Ω) monitored and the light-curve quality (σ_M) generated. The wide-field imager may better serve as a discovery machine leaving the distance determinations to other single-object follow-up instruments.

- Follow-up resources to determine per-SN distances: Supplemental non-LSST follow-up data in the form of improved temporal light-curve sampling (accurate rise and decline times), expanded (UV, NIR) wavelength coverage, and spectral features can access high-fidelity SN Ia models with lower intrinsic magnitude dispersion and residual systematic bias. For example, infrared data (Barone-Nugent et al. 2012) or spectrophotometry at peak brightness (Fakhouri et al. 2015) are projected to give $\sigma_M \lesssim 0.08$ mag. The improvement between $\sigma_M = 0.08$ and 0.15 mag dispersions is equivalent to a factor of 3.52 in number density, or equivalently in survey duration.

- Telescope Aperture $\times$ Exposure Time: Light-collection capabilities depend on the fluxes of the targets. Closer and hence brighter objects require more modest telescope apertures and/or exposure times. For our science case, low-redshift sources are most valuable and the finite amount of follow-up should be spent on saturating redshifts lower than z_{max}.

Focusing on low-redshift supernovae mitigates two important uncertainties associated with the high-z SN Ia cosmology. The measurement is relatively insensitive to absolute color calibration, due to the limited range of *observer*

wavelengths used to standardize restframe distance moduli. Depending on which cameras are used to derive distances, instrumental, as opposed to absolute, calibration may be sufficient. The progenitor population is not expected to evolve significantly in the $0.01 < z < 0.2$ Universe.

4. CONCLUSIONS

SNe Ia are already powerful probes of the homogeneous cosmological expansion of the Universe. In the next decade. high-cadence, wide-field imaging surveys, together with improved precision in their distance determinations, will make SNe Ia powerful probes of the gravity induced-motion caused by the inhomogeneous Universe. SNe Ia peculiar velocities at $z < 0.3$ will measure γ significantly better than galaxy surveys. While imaging surveys will provide a steady stream of SNe Ia, a coordinated plan of follow-up is required to take advantage of their probative power. The resources necessary to follow hundreds of thousands of SNe depend on specific follow-up choices, and access to those resources will define the redshift limits of the survey. Fortunately, the lowest-redshift, and hence brightest, supernovae are of the highest interest. As a point of reference, a practically complete (most fields have disruptive temporal gaps) follow-up survey with $z_{max} = 0.2$ would have $\sim 150,000$, $r \lesssim 20.5$ mag targets over 10 years.

We are interested in

$$F_{00,\alpha}^{-1} = \frac{F_{11,\alpha}}{F_{00}F_{11} - F_{01}^2} - \frac{F_{11}}{(F_{00}F_{11} - F_{01}^2)^2}\left(F_{00,\alpha}F_{11} + F_{00}F_{11,\alpha} - 2F_{01}F_{01,\alpha}\right).$$

$$F_{ij} = \frac{\Omega}{8\pi^2}\int_0^{r_{max}}\int_{k_{min}}^{k_{max}}\int_{-1}^{1} r^2k^2\mathrm{Tr}\left[C^{-1}\frac{\partial C}{\partial\lambda_i}C^{-1}\frac{\partial C}{\partial\lambda_j}\right]d\mu\,dk\,dr \tag{3}$$

$$F_{ij,z} = \frac{\Omega}{8\pi^2}\frac{dr}{dz}r^2\int_{k_{min}}^{k_{max}}\int_{-1}^{1} k^2\mathrm{Tr}\left[C^{-1}\frac{\partial C}{\partial\lambda_i}C^{-1}\frac{\partial C}{\partial\lambda_j}\right]d\mu\,dk$$

$$F_{ij,s} = \frac{\Omega}{8\pi^2}\int_0^{r_{max}}\int_{k_{min}}^{k_{max}}\int_{-1}^{1} r^2k^2\mathrm{Tr}\left[C_{,s}^{-1}\frac{\partial C}{\partial\lambda_i}C^{-1}\frac{\partial C}{\partial\lambda_j} + C^{-1}\frac{\partial C}{\partial\lambda_i}C_{,s}^{-1}\frac{\partial C}{\partial\lambda_j}\right]d\mu\,dk\,dr$$

$$C = \begin{bmatrix} P_{gg}(k,\mu) + \frac{1}{n} & P_{vg}(k,\mu) \\ P_{vg}(k,\mu) & P_{vv}(k,\mu) + \frac{\sigma^2}{n}\end{bmatrix}. \tag{4}$$

$$C_{,n}^{-1} = \frac{n^{-2}((P_{gg}(k,\mu) + \frac{1}{n})\sigma^2 + (P_{vv}(k,\mu) + \frac{\sigma^2}{n}))}{\left((P_{gg}(k,\mu) + \frac{1}{n})(P_{vv}(k,\mu) + \frac{\sigma^2}{n}) - P_{vg}(k,\mu)^2\right)^2} \tag{5}$$

$$\times \begin{bmatrix} P_{vv}(k,\mu) + \frac{\sigma^2}{n} & -P_{vg}(k,\mu) \\ -P_{vg}(k,\mu) & P_{gg}(k,\mu) + \frac{1}{n}\end{bmatrix} \tag{6}$$

$$- \frac{n^{-2}}{(P_{gg}(k,\mu) + \frac{1}{n})(P_{vv}(k,\mu) + \frac{\sigma^2}{n}) - P_{vg}(k,\mu)^2}\begin{bmatrix}\sigma^2 & 0 \\ 0 & 1\end{bmatrix}. \tag{7}$$

$$C_{,\sigma_M}^{-1} = \frac{\ln 10}{5}\frac{z}{1+z}\frac{2\sigma}{n}\Big(\frac{1}{(P_{gg}(k,\mu) + \frac{1}{n})(P_{vv}(k,\mu) + \frac{\sigma^2}{n}) - P_{vg}(k,\mu)^2}\begin{bmatrix}1 & 0 \\ 0 & 0\end{bmatrix} \tag{8}$$

$$- \frac{(P_{gg}(k,\mu) + \frac{1}{n})}{\left((P_{gg}(k,\mu) + \frac{1}{n})(P_{vv}(k,\mu) + \frac{\sigma^2}{n}) - P_{vg}(k,\mu)^2\right)^2} \tag{9}$$

$$\times \begin{bmatrix} P_{vv}(k,\mu) + \frac{\sigma^2}{n} & -P_{vg}(k,\mu) \\ -P_{vg}(k,\mu) & P_{gg}(k,\mu) + \frac{1}{n}\end{bmatrix}\Big) \tag{10}$$

$$\tag{11}$$

REFERENCES

Abate, A., & Lahav, O. 2008, MNRAS, 389, L47, doi: 10.1111/j.1745-3933.2008.00519.x

Adams, C., & Blake, C. 2017, MNRAS, 471, 839, doi: 10.1093/mnras/stx1529

Barone-Nugent, R. L., Lidman, C., Wyithe, J. S. B., et al. 2012, MNRAS, 425, 1007, doi: 10.1111/j.1365-2966.2012.21412.x

Davis, T. M., Hui, L., Frieman, J. A., et al. 2011, ApJ, 741, 67, doi: 10.1088/0004-637X/741/1/67

Fakhouri, H. K., Boone, K., Aldering, G., et al. 2015, ApJ, 815, 58, doi: 10.1088/0004-637X/815/1/58

Gordon, C., Land, K., & Slosar, A. 2007, Phys. Rev. Lett., 99, 081301, doi: 10.1103/PhysRevLett.99.081301

Howlett, C., Robotham, A. S. G., Lagos, C. D. P., & Kim, A. G. 2017a, ApJ, 847, 128, doi: 10.3847/1538-4357/aa88c8

Howlett, C., Staveley-Smith, L., & Blake, C. 2017b, MNRAS, 464, 2517, doi: 10.1093/mnras/stw2466

Hui, L., & Greene, P. B. 2006, PRD, 73, 123526, doi: 10.1103/PhysRevD.73.123526

Huterer, D., Shafer, D. L., & Schmidt, F. 2015, JCAP, 12, 033, doi: 10.1088/1475-7516/2015/12/033

Huterer, D., Shafer, D. L., Scolnic, D. M., & Schmidt, F. 2017, JCAP, 5, 015, doi: 10.1088/1475-7516/2017/05/015

Johnson, A., Blake, C., Koda, J., et al. 2014, MNRAS, 444, 3926, doi: 10.1093/mnras/stu1615

Linder, E. V. 2013, Journal of Cosmology and Astroparticle Physics, 2013, 031

Linder, E. V., & Cahn, R. N. 2007, Astroparticle Physics, 28, 481, doi: 10.1016/j.astropartphys.2007.09.003